

Interaction between conduction band edge and nitrogen states probed by carrier effective-mass measurements in $\text{GaAs}_{1-x}\text{N}_x$

F. Masia, G. Pettinari, A. Polimeni,* M. Felici, A. Miriametro, and M. Capizzi
CNISM and Dipartimento di Fisica, Universita' di Roma "La Sapienza," P.le A. Moro 2, 00185 Roma, Italy

A. Lindsay, S. B. Healy, and E. P. O'Reilly
Tyndall National Institute, Lee Maltings, Cork, Ireland

A. Cristofoli, G. Bais, M. Piccin, S. Rubini, F. Martelli, and A. Franciosi
Laboratorio Nazionale TASC INFN-CNR, Area Science Park, 34012 Trieste, Italy
and Center of Excellence for Nanostructured Materials, University of Trieste, 34127 Trieste, Italy

P. J. Klar, K. Volz, and W. Stolz
Department of Physics and Material Sciences Center, Philipps-University, Renthof 5, D-35032 Marburg, Germany
 (Received 12 May 2005; revised manuscript received 1 December 2005; published 27 February 2006)

The electron effective mass, m_e , has been determined by magnetophotoluminescence in as-grown and hydrogenated $\text{GaAs}_{1-x}\text{N}_x$ samples for a wide range of nitrogen concentrations (from $x < 0.01\%$ to $x = 1.78\%$). A modified $\mathbf{k} \cdot \mathbf{p}$ model, which takes into account hybridization effects between N cluster states and the conduction band edge, reproduces quantitatively the experimental m_e values up to $x \leq 0.6\%$. Experimental and theoretical evidence is provided for the N complexes responsible for the nonmonotonic and initially puzzling compositional dependence of the electron mass.

DOI: [10.1103/PhysRevB.73.073201](https://doi.org/10.1103/PhysRevB.73.073201)

PACS number(s): 78.66.Fd, 71.35.Ji, 71.55.Eq

Incorporation of small percentages ($\sim 1\%$) of nitrogen in III-V compounds and alloys (e.g., GaAs, InGaAs, and GaP) leads to strongly nonlinear modifications in the band structure of the host lattice.¹ One of the most striking effects observed with increasing nitrogen concentration, x , is a large band gap decrease accompanied by a considerable variation in the electron effective mass, m_e (Refs. 1–10). The electron effective mass largely determines the transport and mobility properties of dilute nitrides^{11–13} and is a most critical parameter for testing the various models proposed to explain the peculiar physical properties of these alloys.¹

In an earlier work, it was shown for a limited set of $\text{GaAs}_{1-x}\text{N}_x$ samples and N concentrations that the electron effective mass undergoes a sudden increase around $x = 0.1\%$.⁷ This feature was confirmed by a fine tuning of the nitrogen concentration around this critical value obtained by a post-growth hydrogen irradiation of the samples.⁸ Some of the present authors highlighted by band structure calculations the role played by the interaction between the conduction band (CB) edge and N-related electronic levels in determining the puzzling, abrupt change in the electron effective mass at $x \sim 0.1\%$.¹⁴ A nonmonotonic dependence of the exciton effective mass was also reported around $x = 1.5\%$ in three samples only, and qualitatively ascribed to an interaction between the band edge and N levels.⁶

In this work, we measure by magnetophotoluminescence the electron effective mass for N concentrations ranging from a very dilute limit to a full alloy limit. More than 20 samples, both as-grown and hydrogenated, were investigated in order to get an accurate description of the dependence of m_e on N concentration. After a first abrupt doubling ($m_e \sim 0.13m_0$, where m_0 is the electron bare mass) for $x \sim 0.1\%$,

m_e undergoes a second increase ($\sim 20\%$) for $x \sim 0.35\%$, and finally it shows sizable fluctuations around $m_e \sim 0.14m_0$ for $0.4\% \leq x \leq 1.78\%$. The variation of m_e with x is also calculated by modeling the interaction of the CB edge of $\text{GaAs}_{1-x}\text{N}_x$ with a linear combination of randomly distributed isolated nitrogen states (LCINS model).¹⁴ Excellent agreement is found between experiment and theory up to $x = 0.6\%$. In particular, a crossing between the CB edge and N pair and triplet states accounts for the rapid increase in the electron mass observed respectively at $x \sim 0.1\%$ and $x \sim 0.35\%$. Finally, we find for $x > 0.6\%$ that the model reproduces the experimental data only qualitatively.

We studied $\text{GaAs}_{1-x}\text{N}_x/\text{GaAs}$ thin layer samples grown by molecular beam epitaxy or metal-organic vapor-phase epitaxy having N concentrations $x = 0\%$, $x < 0.01\%$, $x = 0.043$, 0.095 , 0.14 , 0.21 , 0.4 , 0.47 , 0.5 , 0.7 , 0.78 , 1.11 , 1.42 , and 1.78% , as determined by high resolution x-ray diffraction measurements. Most of the samples were irradiated with different hydrogen doses in order to tune finely the N effective concentration (namely, the concentration of N atoms not yet passivated by hydrogen^{8,15}) and trace in detail the dependence of the carrier effective mass on N concentration. Magnetophotoluminescence (magneto PL) was obtained by exciting the samples with the 532 nm line of a vanadate-yttrium aluminum garnet (YAG) laser and by applying a magnetic field (B , up to 12 T) along the $[001]$ growth axis of the samples. The luminescence was dispersed by a $\frac{3}{4}$ m monochromator and detected by a liquid nitrogen-cooled InGaAs linear array. The spectral resolution was 0.1 nm. The theoretical model used in this work was discussed in detail in Ref. 14 and will be summarized in the following.

Figure 1 shows low temperature PL spectra recorded at

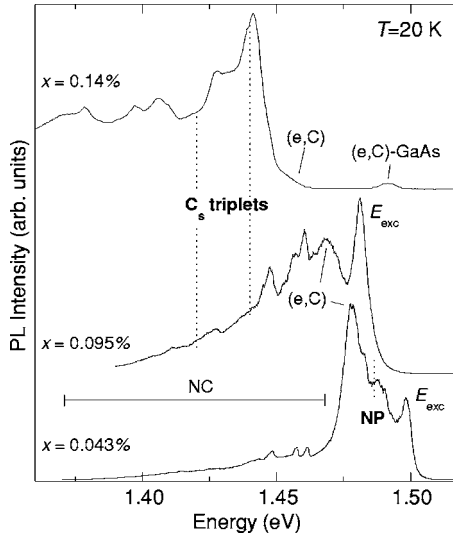


FIG. 1. Photoluminescence spectra of three $\text{GaAs}_{1-x}\text{N}_x$ samples ($x=0.043\%$, 0.095% , and 0.14%) at $T=20$ K. E_{exc} and (e,C) indicate free-exciton recombination, and free-electron to neutral-carbon recombination, respectively. NC labels several recombination bands due to carriers localized on different N clusters. The vertical dashed lines labeled by NP and C_s indicate the *calculated* energy positions of N pairs and triplets, respectively.

$B=0$ T in three representative $\text{GaAs}_{1-x}\text{N}_x$ samples with increasing N concentration. E_{exc} and (e,C) label the recombination of the free-exciton and the free-electron to neutral-carbon recombination in $\text{GaAs}_{1-x}\text{N}_x$, respectively. NC indicates several recombination bands due to carriers localized on different N clusters. In particular, NP and C_s label respectively the *calculated* energy levels of specific N pair and triplets states (their attribution will be discussed in the following). The electron effective mass is derived directly by measuring the slope of the energy shift of the (e,C) recombination with B . Indeed, for sufficiently high fields ($B > 4$ T) this B -induced shift reproduces that of the first Landau level for the electrons,^{7,8} $\Delta E = (\hbar e / 2m_e)B$. The dependence of ΔE on B is shown in Fig. 2 for some characteristic N concentrations, including a 0.043% fully hydrogenated sample whose shift matches that of a N-free GaAs sample.¹⁶ Instead, the bands related to N complexes shown in Fig. 1 do not shift appreciably up to 12 T.

The dependence of the measured electron mass on the nitrogen concentration is shown in Fig. 3, where full circles and diamonds refer to as-grown and hydrogenated samples,¹⁶ respectively. Such dependence displays a rather unusual behavior, which is remarkably reproduced up to $x=0.6\%$ by the theoretical model (open squares in Fig. 3) described below. The red shift of the $\text{GaAs}_{1-x}\text{N}_x$ band gap energy with increasing N concentration was originally accounted for by a two-level band-anticrossing (BAC) model,⁴ where the Γ CB edge of GaAs, ψ_c , interacts with a single nitrogen defect level, ψ_N , which lies above the GaAs CB edge. The $\text{GaAs}_{1-x}\text{N}_x$ CB edge state is then given as $\psi_- = \alpha_c \psi_c + \alpha_N \psi_N$. Since the interaction between the N state and GaAs CB edge, V_N , increases with N composition, the Γ character $f_\Gamma = |\alpha_c|^2$ of the CB edge state of $\text{GaAs}_{1-x}\text{N}_x$ smoothly decreases with

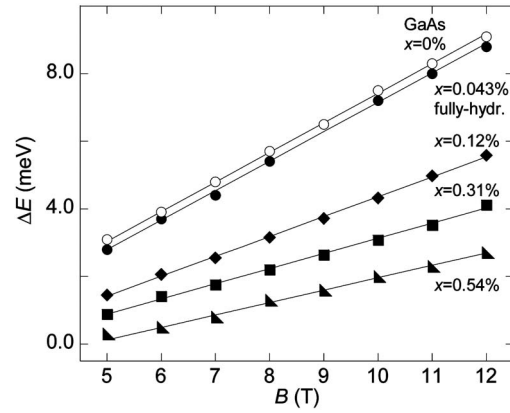


FIG. 2. Magnetic-field induced shift of the (e,C) recombination band for $\text{GaAs}_{1-x}\text{N}_x$ samples as measured at 20 K. Continuous lines are fits to the data through the formula of the first electron Landau level $\Delta E = (\hbar e / 2m_e)B$, where m_e is the only fitting parameter.

x and the electron effective mass varies in a simple $\mathbf{k} \cdot \mathbf{p}$ model as $m_e = (m_c E_{g-}) / (f_\Gamma E_g)$, where E_g and m_c are the GaAs energy gap and effective mass respectively, and E_{g-} is the $\text{GaAs}_{1-x}\text{N}_x$ energy gap. This picture was deeply modified in Ref. 14 to take into account the interaction of the GaAs CB states with a distribution of nitrogen cluster states with energies both above and below the GaAs CB edge.

We model the effects of these clusters by placing $L = 8000 - 10\,000$ nitrogen atoms at random on the group V sites in a $\text{Ga}_M\text{As}_{M-L}\text{N}_L$ supercell with $2M$ total atoms, and with composition $x = L/M$. We use a tight-binding Hamiltonian to calculate the energies ε_l and wave functions ψ_{Nl} ($l = 1, \dots, L$) due to the interactions between the random distribution of nitrogen atoms considered. The strength of the interaction between the GaAs host CB and the l th N-related level is then given by $V_{Nl} = \langle \psi_{Nl} | H | \psi_c \rangle$, with the alloy CB energy levels E_i and wave functions ϕ_i found by diagonalis-

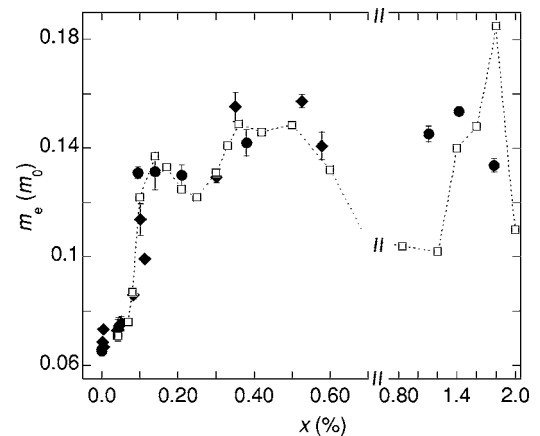


FIG. 3. Measured values of the electron effective mass as a function of the N concentration. Several untreated (full circles) and H-irradiated (full diamonds) samples are considered. Error bars indicate the uncertainty on the mass values (in some case the uncertainty is within the symbol size). Open squares are the calculated effective mass values, the dotted line is a guide to the eye. An abscissa axis break at $x=0.7\%$ is introduced for ease of comparison.

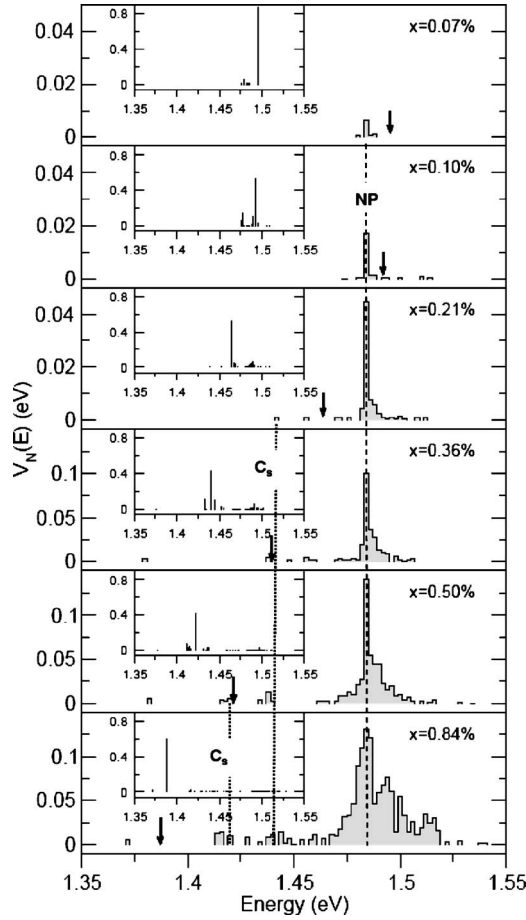


FIG. 4. Calculated distribution of N cluster-state energies ε_l near to the GaAs CB edge, weighted by the square of their interaction $|V_{Nl}|^2$ with the unperturbed conduction band edge wavefunction, ψ_c . Downward vertical arrows show the calculated position of the alloy CB edge energy E_- at each composition x . Dashed and dotted lines mark calculated energies of an isolated N pair (NP) and of C_s triplet states, respectively. Insets show the LCINS spectrum projected onto ψ_c for each composition considered.

ing the $(L+1) \times (L+1)$ Hamiltonian $H_{ij}\phi_i = E_i\phi_i$, where $H_{ll} = \varepsilon_l$, $l=1, \dots, L$; $H_{L+1,L+1} = E_c$, and $H_{l,L+1} = H_{L+1,l} = V_{Nl}$. For increasing N concentration, the $\text{GaAs}_{1-x}\text{N}_x$ CB edge redshifts and crosses the different N cluster levels. Depending both on the energy of the CB edge relative to the cluster state energies, ε_l , and also on the magnitude of V_{Nl} for each state, f_Γ will change in a *nonmonotonic* way, and so too will the electron effective mass, as discussed further in Ref. 14.

The close agreement between the theoretical and experimental values of m_e shown in Fig. 3 will be discussed in detail now. The histograms in Fig. 4 display the calculated evolution with N concentration of the interaction $V_N(E)$ between the GaAs CB edge and the N defect states at energies ε_l close to the $\text{GaAs}_{1-x}\text{N}_x$ CB edge, where $V_N(E)$ is given by

$$V_N(E) = \sum_l |V_{Nl}|^2 T(E - \varepsilon_l),$$

with $T(x)$ a top-hat function of width 2 meV and unit area. The vertical downward-pointing arrow in each panel shows

the calculated position of the $\text{GaAs}_{1-x}\text{N}_x$ CB edge, E_- , for that value of x . The insets show the alloy energy spectrum, $G_\Gamma(E) = \sum_i |\langle \phi_i | \psi_c \rangle|^2 \delta(E - E_i)$ projected onto the GaAs Γ CB edge state ψ_c . E_- is defined as the state with largest Γ character, $|\langle \phi_i | \psi_c \rangle|^2$ in each inset panel.

At $x=0.07\%$, E_- is above the energy of N pair (NP) states formed by a single Ga and two first neighbor N atoms and located 1.486 eV above the valence band maximum. Correspondingly, the inset shows that the E_- level interacts only weakly with the relatively small number of N pair levels. As a result the CB edge retains a large Γ character, $f_\Gamma=0.87$, and the electron effective mass value is close to that predicted by the two-level BAC model. For $x=0.1\%$ and 0.21% , E_- moves downwards, through the N pair levels whose density is increasing quickly, approximately as x^2 . The CB edge hybridizes with these states, as indicated by the distribution of the Γ character across a band of states below (above) the E_- level for $x=0.1\%$ (0.21%), and the E_- level Γ character decreases down to $f_\Gamma=0.54$ (0.52). In turn, m_e increases with respect to the values predicted by the two-level BAC model and well matches both the values and trend of the experimentally determined m_e ; see Fig. 3.

For $x > 0.21\%$, an extrapolation of the low x data in Fig. 3 might suggest a decrease in m_e towards the two-level BAC value. However, the density of low-energy N-related states starts to increase markedly with increasing x , as shown in Fig. 4. The states located at about 1.42–1.44 eV are due to C_s triplets, a noncoplanar chain of N-Ga-N-Ga-N atoms having reflective symmetry only, whose density initially increases very quickly, approximately as x^3 . For $x=0.36\%$ and 0.5% , the E_- level interacts strongly with these C_s -related levels, with a weaker interaction still observed with the N-N pair levels whose distance in energy from the E_- level increases with x . These combined interactions lead to a further reduction in f_Γ , consistent with the additional, sudden increase in m_e observed experimentally in Fig. 3 in this concentration range. At higher N concentration and over a small composition range, the E_- level lies in a gap between the calculated N-related defect levels, as illustrated for $x=0.84\%$ in Fig. 4. The value of f_Γ increases in this N concentration range, leading to a predicted reduction in m_e over a small range of x .

At higher N concentration, the quantitative match between theoretical and experimental values of m_e , which includes the two jumps at $x=0.1\%$ and 0.35% , is lost and only the scatter in the experimental data is qualitatively reproduced. This may reflect several factors including: (i) the relatively small number of experimental data points in this range;¹⁷ (ii) that the higher composition samples may not be perfectly random disordered alloys, as assumed in the LCINS calculations;¹⁸ (iii) that the LCINS calculations omit some relevant but statistically rare clusters, or (iv) that the accuracy of the LCINS parametrization may decrease for the larger N clusters which contribute to the LCINS spectrum at lower energies ($E < 1.4$ eV).

A direct experimental evidence of the N cluster states invoked by the theory to account for the two jumps in m_e is here provided. First, the band gap of $\text{GaAs}_{1-x}\text{N}_x$ is estimated to be at 1.491 eV for $x=0.1\%$, namely, where the first steep

increase in m_e is observed in Fig. 3. This energy value is very close to the *calculated* energy of the NP level (1.486 eV, see Fig. 4) and to the peak energy (1.488 eV) of a band observed in the emission spectrum of the $x=0.043\%$ sample (see Fig. 1, label NP). Second, the band gap of $\text{GaAs}_{1-x}\text{N}_x$ for $x=0.36\%$, where the second m_e jump is observed in Fig. 3, is estimated to be at 1.435 eV. This value falls in the energy range where two N triplet states have been found theoretically (1.42 eV and 1.44 eV, see Fig. 4), and nicely agrees with the energy of the doubly peaked emission observed in the PL spectra of the 0.14% sample (C_5 label in Fig. 1). Therefore, the abrupt changes we observe in the measured values of m_e can be ascribed to the crossing of the CB edge with N pair and triplet states, as predicted by the theory. Finally, one may argue that the other N states visible in the PL spectra are either not effective as far as the interaction with the CB edge and ensuing m_e increase is concerned, or are responsible for the lack of observation of the mass decrease, which is predicted to occur at $x \sim 1\%$.

Before concluding, it is worth noticing that the above considerations should not apply to $\text{In}_y\text{Ga}_{1-y}\text{As}_{1-x}\text{N}_x$. In this case, the incorporation of In shifts the CB edge away from N

complex states that should not vary their energy position sizably, thus weakening the interaction between extended and N localized states. In fact, a conventional $\mathbf{k}\cdot\mathbf{p}$ -based band anticrossing model¹⁹ well reproduces the compositional dependence of the electron effective mass for $0.1 < y < 0.4$.^{9,10}

In conclusion, a quite puzzling dependence of the carrier effective mass on N concentration has been experimentally measured and quantitatively matched by a theoretical model including the perturbation induced by N clusters on the CB edge in dilute nitrides. In particular, a strong perturbation has been found to affect the electron effective mass when the downward moving CB edge of $\text{GaAs}_{1-x}\text{N}_x$ crosses specific N pair and triplet states in the gap, whose evidence has been provided by experiment and theory, as well.

A.P. and P.J.K. acknowledge, respectively, Ministero dell'Universita' (Italy) and Deutscher Akademischer Austauschdienst (Germany) for funding through Vigoni Programme. EOR acknowledges support from Science Foundation Ireland.

*Corresponding author. Email address: polimeni@roma1.inf.it

¹For a review, see *Physics and Applications of Dilute Nitrides*, edited by I. A. Buyanova and W. M. Chen (Taylor & Francis Books Inc., New York, 2004), and *Dilute Nitride Semiconductors*, edited by M. Henini (Elsevier, Oxford, 2005).

²Y. Zhang, A. Mascarenhas, H. P. Xin, and C. W. Tu, *Phys. Rev. B* **61**, 7479 (2000).

³P. N. Hai, W. M. Chen, I. A. Buyanova, H. P. Xin, and C. W. Tu, *Appl. Phys. Lett.* **77**, 1843 (2000).

⁴J. Wu, W. Shan, W. Walukiewicz, K. M. Yu, J. W. Ager, III, E. E. Haller, H. P. Xin, and C. W. Tu, *Phys. Rev. B* **64**, 085320 (2001).

⁵D. L. Young, D. L. Geisz, and T. J. Coutts, *Appl. Phys. Lett.* **82**, 1236 (2003).

⁶Y. J. Wang, X. Wei, Y. Zhang, A. Mascarenhas, H. P. Xin, Y. G. Hong, and C. W. Tu, *Appl. Phys. Lett.* **82**, 4453 (2003).

⁷F. Masia, A. Polimeni, G. Baldassarri Höger von Högersthal, M. Bissiri, M. Capizzi, P. J. Klar, and W. Stolz, *Appl. Phys. Lett.* **82**, 4474 (2003).

⁸A. Polimeni, G. Baldassarri Höger von Högersthal, F. Masia, A. Frova, M. Capizzi, S. Sanna, V. Fiorentini, P. J. Klar, and W. Stolz, *Phys. Rev. B* **69**, 041201(R) (2004).

⁹G. Baldassarri Höger von Högersthal, A. Polimeni, F. Masia, M. Bissiri, M. Capizzi, D. Gollub, M. Fischer, and A. Forchel, *Phys. Rev. B* **67**, 233304 (2003).

¹⁰A. Polimeni, F. Masia, G. Baldassarri Höger von Högersthal, and

M. Capizzi, in *Dilute Nitride Semiconductors*, edited by M. Henini (Elsevier, Oxford, 2005), p. 223.

¹¹J. Teubert, P. J. Klar, W. Heimbrodt, K. Volz, W. Stolz, P. Thomas, G. Leibiger, and V. Gottschalch, *Appl. Phys. Lett.* **84**, 747 (2004).

¹²S. Fahy and E. P. O'Reilly, *Appl. Phys. Lett.* **83**, 3731 (2003).

¹³D. Fowler, O. Makarovskiy, A. Patane', L. Eaves, L. Geelhaar, and H. Riechert, *Phys. Rev. B* **69**, 153305 (2004).

¹⁴A. Lindsay and E. P. O'Reilly, *Phys. Rev. Lett.* **93**, 196402 (2004).

¹⁵A. Polimeni, G. Baldassarri Höger von Högersthal, M. Bissiri, M. Capizzi, M. Fischer, M. Reinhardt, and A. Forchel, *Phys. Rev. B* **63**, 201304(R) (2001).

¹⁶For hydrogenated samples, x is derived by inverting the relation obtained by fitting the band gap exciton energy of the as-grown samples as $E_{\text{exc}}(x) = E_{\text{exc}}^{\text{GaAs}} - A \cdot x^\beta$, where $E_{\text{exc}}^{\text{GaAs}}$ is the free-exciton energy in GaAs, $A=0.23$ eV, and $\beta=0.86$.

¹⁷ $m_e=0.19m_0$ has been measured in a $\text{GaAs}_{0.98}\text{N}_{0.02}$ quantum well, see Ref. 3, a value of similar magnitude to that predicted here by the LCINS model for $x=1.8\%$.

¹⁸N solubility is much lower in GaAs than that frozen in our samples by the epitaxial growth. Moreover, phase segregation and clustering effects impede to grow good $\text{GaAs}_{1-x}\text{N}_x$ samples with N concentration higher than 5%.

¹⁹Stanko Tomic and Eoin P. O'Reilly, *Phys. Rev. B* **71**, 233301 (2005).